Oxygen Permeation Properties and Phase Stability of Co-Free La$_{0.6}$Sr$_{0.4}$Ti$_{0.2}$Fe$_{0.8}$O$_{3-\delta}$ Oxygen Membrane

Ki Young Kim, Jung Hoon Park[†], Jong Pyo Kim, Sou Hwan Son, and Sang Do Park[*]

Energy Conversion Research Department, Korea Institute of Energy Research, 71-2, Jang-dong, Yuseong-gu,
Daejeon 305-343, Korea

*Carbon Dioxide Reduction and Sequestration R&D Center, Korea Institute of Energy Research, 71-2, Jang-dong, Yuseong-gu,
Dajeon 305-343, Korea

Abstract: A perovskite-type (La$_{0.6}$Sr$_{0.4}$Ti$_{0.2}$Fe$_{0.8}$O$_{3-\delta}$) dense ceramic membrane was prepared by polymerized complex method, using citric acid as a chelating agent and ethylene glycol as an organic stabilizer. Effect of Ti addition on lanthanum-strontium ferrite mixed conductor was investigated by evaluating the thermal expansion coefficient, the oxygen flux, the electrical conductivity, and the phase stability. The thermal expansion coefficient in air was 21.19×10^{-6}/K at 473 to 1,223 K. At the oxygen partial pressure of 0.21 atm (20% O$_2$), the electrical conductivity increased with temperature and then decreased after 973 K. The decrement in electrical conductivity at high temperatures was explained by a loss of the lattice oxygen. The oxygen flux increased with temperature and was 0.17 mL/cm$^2 \cdot$ min at 1,223 K. From the temperature-dependent oxygen flux data, the activation energy of oxygen ion conduction was calculated and was 80.5 kJ/mol at 1,073 to 1,223 K. Also, the Ti-added lanthanum-strontium ferrite mixed conductor was structurally and chemically stable after 450 hours long-term test at 1,173 K.

1. Introduction

Mixed conducting membranes possessing oxygen ionic and electronic conductivities have been interested due to their oxygen separation ability. Especially, the ceramic dense membrane has a great potential to be applicable in chemical and petroleum industries for oxygen separation from oxygen mixture gas. It is very attractive technology economically and environmentally in industrial process with hot-turbine system [1,2].

Perovskite type oxides substituted with lower valence cations and transition metals at A and B sites of ABO3-Perovskite structure respectively showed improving el-

ectrical conductivity and ionic conductivity. The improvements leads to high oxygen permeability of dense ceramic perovskite type membrane of La(Sr)Fe(Co) that have been studied by many researchers [3-8], since Teraoka *et al.* [9] reported first about SrCo$_{0.8}$Fe$_{0.2}$O$_{3-\delta}$. Many researches have been deal with the new material with high oxygen permeability, and good stability at high temperatures and reducing conditions. In a feasibility test, Bredesen and Sogge [10] reported that a minimum oxygen permeation flux should be 10 mL/cm$^2 \cdot$ min to adapt commercially in viable processes to have advantage with other traditional processes. Oxygen permeation of membranes can be improved by modification of many characteristics such as composition of membrane, membrane thickness, microstructure and temperature at the condition where the membranes

[†]Author for all correspondences
(e-mail : pjhoon@kier.re.kr)

should be applied. Among these properties, the membrane material and composition are intrinsic factor to obtain good enough oxygen flux to be applied. It is well known that different components can cause different oxygen permeation fluxes [11]. The influence of substitution of A site on oxygen permeation properties in the system of La(A)CoFeO$_{3-\delta}$ (A = Sr, Ba, Ca) was investigated by Stevenson et al. [11] and Tsai et al. [13]. Based on these results, although the oxygen permeation flux is inclined to increase as increasing A-site substitution with lower valence atom than host atom, the phase stability became unstable in the low oxygen partial pressure and high temperature environment. High Sr contents are associated with poorer dimensional stability under the large oxygen chemical potential gradients [14,15]. Thermal expansion coefficients of membrane containing Co elements are usually higher than that of other ceramic materials [16,17]. For instant, LSCF series possessed thermal expansion coefficients, $20 \sim 26 \times 10^{-6}$/K, in the temperature region, $973 \sim 1,273$ K. Nevertheless, La$_{0.6}$Sr$_{0.4}$Co$_{0.2}$Fe$_{0.8}$O$_{3-\delta}$ has been promising material for oxygen-separating membrane among the membrane containing Co elements. Only long term stability was question so as to commercialize, especially in oxidizing and reducing condition [18,19]. To improve stability under reducing and oxidizing conditions, the partially substituting Co with more redox-stable cations such as chromium and titanium can be answer. However, Cr had the polarizing nature of the dopant causing substantial lower ionic conductivity [20]. On the other hand, moderate additions of titanium were found to suppress to some extent the ordering processes in the oxygen sublattice of LaSr(Fe,Ti)O$_{3-\delta}$ phases, with the highest ionic transport under oxidizing conditions observed for a composition with 20% titanium on the Fe site [21].

In this work, Co elements in La$_{0.6}$Sr$_{0.4}$Co$_{0.2}$Fe$_{0.8}$O$_{3-\delta}$ were substituted with Titanium to improve long-term phase stability and reduce thermal expansion coefficient. La$_{0.6}$Sr$_{0.4}$Ti$_{0.2}$Fe$_{0.8}$O$_{3-\delta}$, LSTF6428 perovskite type oxides has been synthesized using polymerized complex method which can synthesizes a homogeneous and pure powder relatively low sintering temperature. The purpose of this work was to investigate the fundamental properties of La$_{0.6}$Sr$_{0.4}$Ti$_{0.2}$Fe$_{0.8}$O$_{3-\delta}$, LSTF6428, including the electrical conductivity depending on oxygen partial pressure, and oxygen permeation property. Long-term phase stability was also studied by using XRD.

2. Experimental Procedure

2.1. Sample Preparations

Polymerized complex method usually used a complexation like citric acid that converted metal ions to metal-chelates complex, which can be stabilized in ethylene glycol with being dispersed homogeneously. Heating the solution around $393 \sim 423$ K, the solution became polymer through the polymerization due to successive esterification reaction. Dispersed the metal chelates in solution became immobilized and polymerized homogeneously at first mixing condition. After thermal decomposition, homogeneous and pure complicate oxide materials were obtained from the polymer.

To synthesize the purposed composition, reagent grade La(NO$_3$)$_2 \cdot$ 6H$_2$O (99.99%, Aldrich, USA), Sr(NO$_3$)$_2$ (99%, Aldrich, USA), Fe(NO$_3$)$_3 \cdot$ 9H$_2$O (99%, Aldrich, USA), Ti[OCH(CH$_3$)$_2$]$_4$ (97%, Aldrich, USA), ethylene glycol (99.5% DC chemical, Korea) and citric acid (99.5%, SAMCHUN, Korea) were used as starting materials. The chemical of Ti-source added and dissolved into ethylene glycol solution on the hot plate at 353 K. After obtaining transparent solution, Citric acid added into the solution. After citric acid dissolved completely, Sr and La added into ethylene glycol and citric acid solution. Until the solution became transparent on a hot plate at 403 K, it mixed continuously. For esterification reaction, after that, the temperature of hot plate raised up to 473 K with stirring for 12 h. After the condensation, the polymer burned out for thermal decomposition at 723 K in metal heater. The obtained precursor was heated thermally at 1,073 K for
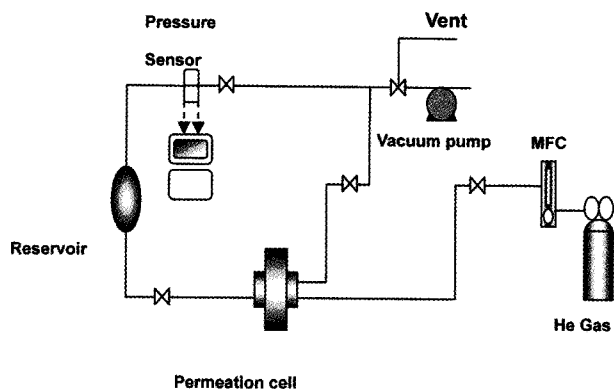
Fig. 1. The schematic diagrams of He-gas tightness test.

Fig. 2. The schematic diagrams of permeation test cell.

2 h to remove residual carbon and impurity in air. The as-synthesized powders were compressed into disks of 20 mm in diameter and 1.0~2.0 mm of thickness in a stainless steel mold under a hydraulic load of 9 ton on an area of 5.07 cm^2 by unilateral press (model 25601 series, Specac Limited, U.K.). The green disk sintered at 1,573 K for 5 h. The sintered disk was polished with 600 grit SiC on both surfaces by Grinder (Beta series, Buehler LTD., U.S.A) to smooth the surface and to control the thickness of disk. After that, the disk was cut into proper rectangular bars to measure electrical conductivity.

2.2. Analyses of Powder and Membrane

The phase of the powder and the disk before and after sintering were characterized with an X-ray diffractometer (XRD, Rigaku Co Model D/Max 2200-Ultimaplus, Japan) using CuKα radiation in the Bragg angle range $20° < 2\theta° < 80°$. To measure electrical conductivity, the rectangular specimen was painted with silver paste. The oxygen partial pressure dependence of electrical conductivity was measured by DC four-probe method using Reference 600TM (Gamry instruments, USA) with a flow rate 100 mL/min at 1,173 K. Dilatometer was used to measure the thermal expansion coefficients with the temperature region, 473~1,273 K, heating rate 1 K/min.

2.3. He-gas Tightness Test of Membrane

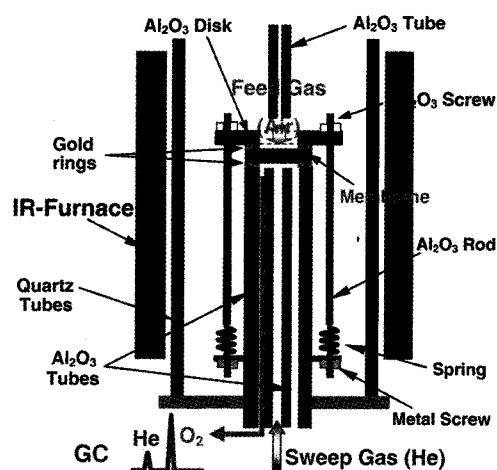Gas tightness was measured with unsteady state gas

permeation setup. Fig. 1 shows the schematic diagram of He gas-tightness test.

He gas-tightness test of as-prepared membrane (La$_{0.6}$Sr$_{0.4}$Ti$_{0.2}$Fe$_{0.8}$O$_{3-\delta}$, LSTF6428) was conducted at room temperature. The membrane and rubber o-ring are assembled and the permeation side of the whole assembly cell was vacuumed with vacuum pump to be zero (absolute pressure). The pressure change of permeation side was monitored, whilst helium gas was supplied into feeding side. If the pressure maintained within error range for 1 h, the membrane was recognized as gas tightness.

2.4. Oxygen Permeation Measurement

The membrane permeation cell test parts used in this work is shown in Fig. 2.

A disk type permeation cell was used in this work for oxygen permeation study. Au ring (Au plate, 99.9 %, Aldrich) was used as the sealant material to seal the disk onto the dense alumina tube. Prior to oxygen permeation test, the cell part was purged with He gas to remove the air in permeation cell tube and to confirm the sealing onto the assembly consisted of alumina tubes, membrane and sealant for 20 h. The leakage test for the outer parts of apparatus such as line, fitting and valve was conducted with supplying N$_2$ gas at feed side. Permeation study was performed within the temperature range of 1,023~1,123 K. The temperature
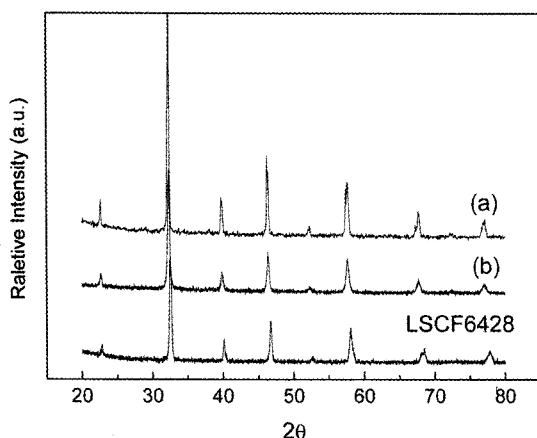
Fig. 3. X-ray diffraction patterns of $La_{0.6}Sr_{0.4}Ti_{0.2}Fe_{0.8}O_{3-\delta}$, (a) after sintering at 1,573 K for 5 h, (b) treating thermally at 1,073 K for 2 h, comparing with that of $La_{0.6}Sr_{0.4}Co_{0.2}Fe_{0.8}O_{3-\delta}$ sintered at 1,573 K for 5 h.

of the cell was increased up to 1,123 K, with a heating rate of 1.5 K/min and holing at desired temperature for 100 min to attain steady state condition of gas flow. Synthesis air (21 vol.% O_2 + 79 vol.% N_2) and pure He (99.999%) were introduced into the different side of the membrane disk, which were controlled by the mass flow controller (MKS 247C). The feed flow rate was kept at 20 mL/min, and sweep flow rate was 20 mL/min on the permeated side. The oxygen content in the permeate stream was measured with a gas chromatograph (GC-TCD, Acme 6000, YoungLin, Korea). Helium was used as a reference gas, and a 1.8 m − 5 Å molecular sieves was employed for gas separation. The gas chromatograph equipped with an automated sampling pump was used to analyze both oxygen and nitrogen concentration of sweep side. The gas chromatograph was frequently calibrated by using standard gas mixture of oxygen and nitrogen in helium in order to ensure reliability of the experimental data.

3. Results and Discussion

3.1. Sample Preparation and Characterization

Fig. 3 showed XRD patterns of $La_{0.6}Sr_{0.4}Ti_{0.2}Fe_{0.8}O_{3-\delta}$, (LSTF6428) in calcinations at 1,073 K for 2 h and sintering at 1,573 K for 5 h, for the comparison,

$La_{0.6}Sr_{0.4}Co_{0.2}Fe_{0.8}O_{3-\delta}$, (LSCF6428) sintered at 1,573 K for 5 h.

It was confirmed that single-phase perovskite structure was already obtained even at calcinations temperature by XRD. XRD patterns of LSTF6428 are similar with LSCF6428, having the same number of peaks in the observing 2θ region. However, the observed XRD peaks in LSTF6428 slightly shifted to lower angle than that of LSCF6428. The substitution of smaller ionic radius Ti^{4+}, 0.88 Å [22] at CN = 8 than that of Co^{2+}, 1.04 Å at CN = 8 into Co element results in decreasing of the averaged radius of B atoms, which leads to decrease the unit cell volume of ABO_3 perovskite structure. The XRD result of the substitution of smaller ionic radius atoms usually let peaks shift to higher angle. However, our XRD patterns showed opposite result; the observed XRD peaks in LSTF6428 slightly shifted to lower angle than that of LSCF6428, which means the unit cell volume of LSTF6428 became larger than that of LSCF6428, even though the substituted Ti ion has smaller ionic radius than Co ion. The transition metal ions such as Co and Fe ions oxidized to form Co^{3+} and Fe^{4+} in order to maintain electrical neutrality from the charge imbalance caused by substitution of Sr^{2+} ions into La^{3+} ions in LSCF6428 [7]. According to the Pauling's rules, when Co^{2+} and Fe^{3+} ions transited to the trivalent or tetravalent ions, it will strengthen B-O bonds in the BO_6 in the perovskite lattice. As a result, the volume of the unit cell will decrease. In our case, redox-stable cations and tetravalence Ti^{4+} acted a role to prevent Fe^{3+} from converting tetravalence Fe^{4+}, in other word, 20% Ti substitution prevented Fe oxidation to some extent enough to become larger unit cell than LSCF6428, based on the XRD results. It indicated that LSTF6428 could be more stable than LSCF in oxidizing and reducing condition, even if the concentration of electron-hole pairs caused by substitution of Sr^{2+} ions into La^{3+} ions in LSTF6428 would decrease.

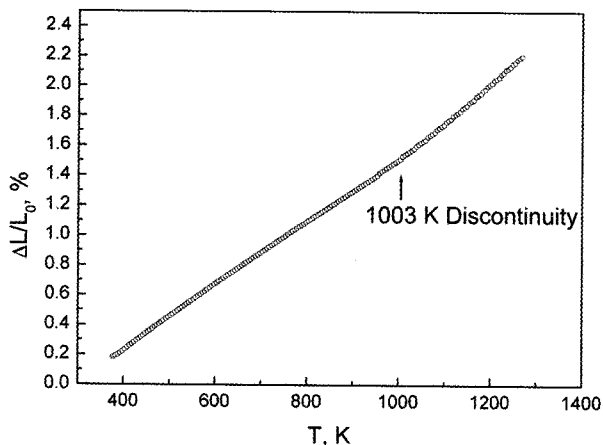Dilatometric curve of LSTF6428 measuring in the temperature region between 473 and 1,273 K in air

Fig. 4. Dilatometric curves of the $La_{0.6}Sr_{0.4}Ti_{0.2}Fe_{0.8}O_{3-\delta}$, arrow indicated the discontinuity of thermal expansion coefficient in air.

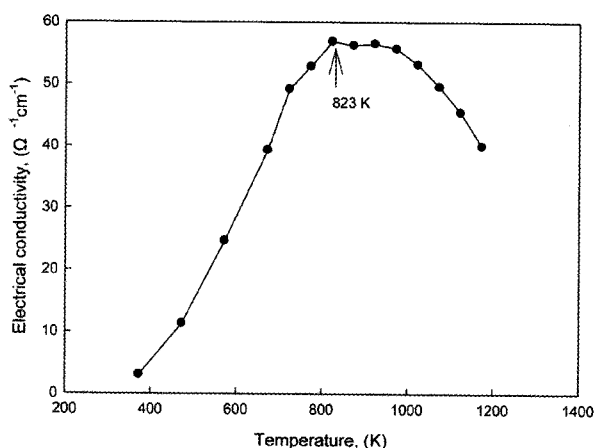**Fig. 5.** Electrical conductivity (σ) versus absolute temperature T (K) of $La_{0.6}Sr_{0.4}Ti_{0.2}Fe_{0.8}O_{3-\delta}$ membrane sintered at 1,573 K for 5 h.

shows in Fig. 4.

The discontinuity was observed at 1,003 K in dilatometirc curve. The calculated thermal expansion coefficients of $La_{0.6}Sr_{0.4}Ti_{0.2}Fe_{0.8}O_{3-\delta}$ were 21.19×10^{-6}/K from 473 to 1273 K. The increase of thermal expansion coefficient in high temperature region is caused by chemically-induced expansion of the lattice due to oxygen loss [21]. It indicates that the temperature starting oxygen loss in sub-lattice is around 973 K. The Ti-substitution results in considerable decrease of thermal expansion coefficient comparing with LSCF6428, 26×10^{-6}/K at high temperature region above 973 K.
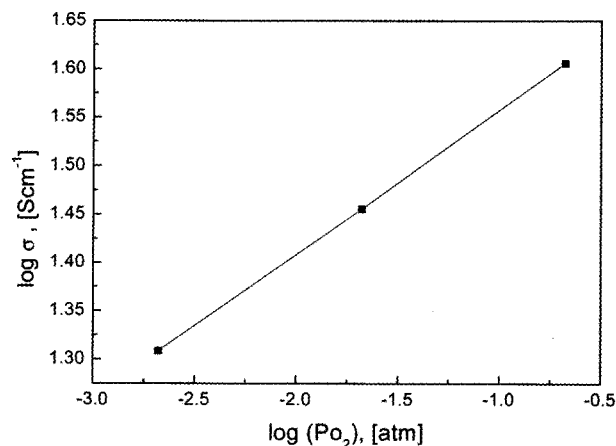

Fig. 6. Po_2 dependence of the electrical conductivity of $La_{0.6}Sr_{0.4}Ti_{0.2}Fe_{0.8}O_{3-\delta}$ at 1,173 K.

3.2. Electrical Conductivity

Fig. 5 shows the electrical conductivity of $La_{0.6}Sr_{0.4}Ti_{0.2}Fe_{0.8}O_{3-\delta}$ sintered at 1,573 K for 5 h in air.

The electrical conductivities of the $La_{0.6}Sr_{0.4}Ti_{0.2}Fe_{0.8}O_{3-\delta}$ increased to a maximum conductivity at 823 K, kept plateau until 923 K, and then decreased from 1,003 K that is consistent with the temperature showing discontinuity in dilatometric curve in Fig. 4. It indicates the loss of oxygen in sub-lattice for compensating charge carriers from the resulting in formation of oxygen vacancies in the high temperature region appeared to start at 1,003 K. Kim *et al.* [23] explained this temperature dependence with two competitive factors; one is electronic compensation of charge disproportion of transition metal ions (Fe^{3+} ions into Fe^{4+}) and the other is the ionic compensation of oxygen vacancy formation. The phenomenon of electric conductivity depending on temperature might relate with the oxygen losses that reduce the charge carriers generated from acceptor (Sr) dopants.

The dependence of electrical conductivity on oxygen partial pressure between 2×10^{-3} and 0.21 atm at 1,173 K, shown in Fig. 6.

Electric conductivity LSTF6428 increased with increase of oxygen partial pressure. This is typical behavior of p-type conduction (electron hole, $h^{\cdot}$). The experimental measurement of ln (σ) for $La_{0.6}Sr_{0.4}Ti_{0.2}Fe_{0.8}O_{3-\delta}$
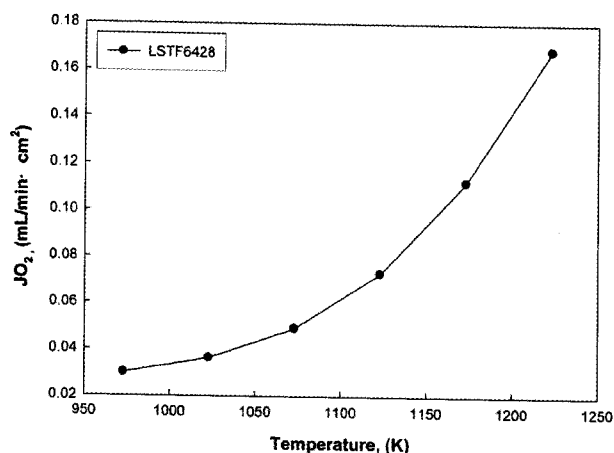
Fig. 7. Temperature dependence of oxygen permeation flux of La$_{0.6}$Sr$_{0.4}$Ti$_{0.2}$Fe$_{0.8}$O$_{3-\delta}$ membrane at partial pressure of 0.21/1 × 10^{-5} atm (helium flow rate: 20 mL/min).

at 1,173 K showed $\approx$ -1/6 dependence of ln (Po$_2$) within Po$_2$ range between 2 × 10^{-3} to 0.21 atm. This electric conductivity dependence on oxygen partial pressure suggests doubly-ionized oxygen vacancies. When the oxygen vacancy is doubly ionized at elevated temperature, thermal dissociation of the oxygen in sublattice occurs into oxygen vacancies with electron or ionized oxygen vacancies. The possible defect equation and relation in equilibrium condition can be considered with following ;
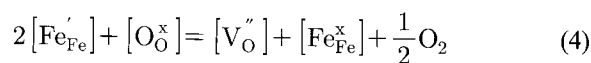
$$[O_O^x] = [V_O^{''}] + [Fe_{Fe}^x] + \frac{1}{2}O_2 \qquad (1)$$

$$[V_O^{''}] = P_{O_2}^{1/6} \exp\left(\frac{-\Delta H}{3RT}\right) \qquad (2)$$

$$\ln[V_O^{''}] \approx \frac{1}{6}\ln P_{O_2} \qquad (3)$$

where ΔH represented standard enthalpy change of re-

action (1). Consequently, the equilibrium between oxygen in La$_{0.6}$Sr$_{0.4}$Ti$_{0.2}$Fe$_{0.8}$O$_{3-\delta}$ and oxygen in the gas phase at 1,173 K can be stated by following relationship.

$$2[Fe_{Fe}^{'}] + [O_O^x] = [V_O^{''}] + [Fe_{Fe}^x] + \frac{1}{2}O_2 \qquad (4)$$

3.3. Oxygen Permeability

The oxygen permeation study was performed La$_{0.6}$Sr$_{0.4}$Ti$_{0.2}$Fe$_{0.8}$O$_{3-\delta}$, after sealing test with gold ring at 1,336 K. Oxygen in equipment is removed by introducing N$_2$ as purge gas, and then helium and air were introduced to the lines. After the introduction of helium, the oxygen partial pressure gradient generated gradually onto both sides of the membrane from high oxygen partial pressure (air side, Po$_2$ = 0.21 atm, feed side) to low oxygen partial pressure (He sweep side, permeated side). The oxygen permeation flux through a disk type dense membrane of La$_{0.6}$Sr$_{0.4}$Ti$_{0.2}$Fe$_{0.8}$O$_{3-\delta}$ with 1.6 mm thickness was measured in the temperature range between 973 and 1,223 K. Fig. 7 shows the oxygen permeation flux for dense membrane La$_{0.6}$Sr$_{0.4}$Ti$_{0.2}$Fe$_{0.8}$O$_{3-\delta}$ as function of temperature.

The oxygen permeation flux was increased with temperature exponentially. The measured oxygen permeation flux was 0.17 mL/min · cm^2 at 1,223 K. For the comparison, the oxygen permeation fluxes of La$_{0.5}$Sr$_{0.5}$FeO$_{3-\delta}$ and La$_{0.5}$Sr$_{0.5}$Ti$_{0.1}$Fe$_{0.9}$O$_{3-\delta}$ [20,21] shows in Table 1.

Taking into account thickness of the membrane, our oxygen permeation flux was similar with that of La$_{0.5}$Sr$_{0.5}$Ti$_{0.1}$Fe$_{0.9}$O$_{3-\delta}$ reference data, but lower than that of La$_{0.5}$Sr$_{0.5}$FeO$_{3-\delta}$ without Ti. Ti-substitution did not help to improve oxygen permeation properties be-

Table 1. Oxygen Permeation Flux Data of Various Co Free Perovskite Type Membranes

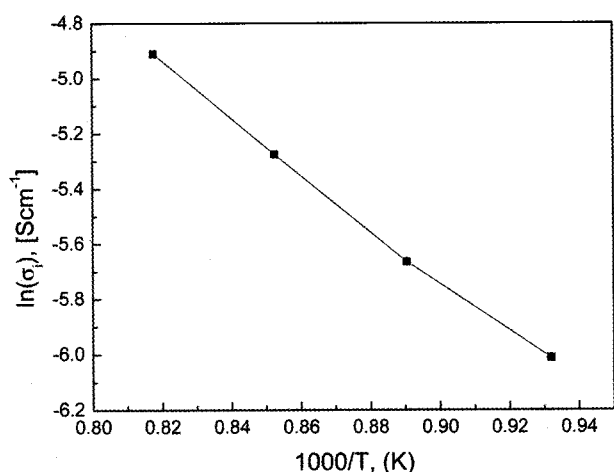| Membrane composition	Temperature, (K)	Thickness	Oxygen permeation flux
La$_{0.6}$Sr$_{0.4}$Ti$_{0.2}$Fe$_{0.8}$O$_{3-\delta}$, in our experiment	1,223	1.6 mm	0.17 mL/min · cm^2
La$_{0.3}$Sr$_{0.7}$Cr$_{0.2}$Al$_{0.3}$Fe$_{0.5}$O$_{3-\delta}$, [18]	1,173	1 mm	0.05 mL/min · cm^2
La$_{0.5}$Sr$_{0.5}$FeO$_{3-\delta}$, [19]	1,223	1 mm	0.39 mL/min · cm^2
La$_{0.5}$Sr$_{0.5}$Ti$_{0.1}$Fe$_{0.9}$O$_{3-\delta}$, [19]	1,223	1 mm	0.21 mL/min · cm^2

Fig. 8. Arrhenius plot of the ionic conductivity calculated from the oxygen permeation flux of the $La_{0.6}Sr_{0.4}Ti_{0.2}Fe_{0.8}O_{3-\delta}$ membrane.
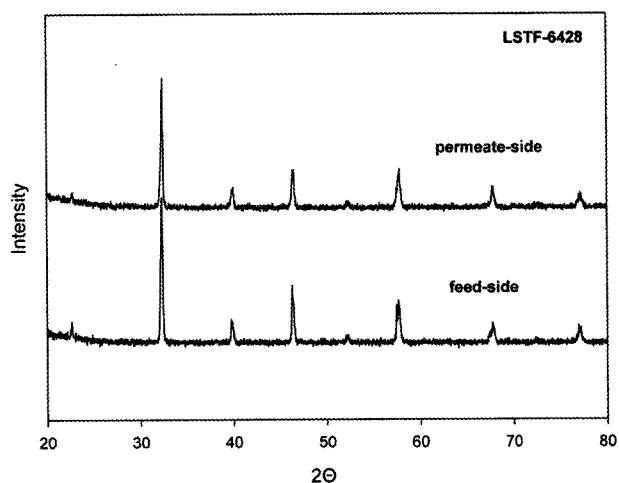

Fig. 9. X-ray diffraction patterns of permeation side and feed side of $La_{0.6}Sr_{0.4}Ti_{0.2}Fe_{0.8}O_{3-\delta}$ membrane after oxygen permeation test.

cause tetravalent Ti^{4+} reduced the charge carrier concentration generated from substitution of Sr^{2+} ions into La^{3+} ions in LSTF6428, which evidence was shown in XRD pattern shifting to lower angle, even smaller ionic radius Ti^{4+} was substituted with.

Ionic conductivities were calculated from the measured oxygen permeation flux by using the following relation (5) [12].

$$\sigma_i = (4\,FJt)\left(RT\ln\left[P\left(O_2^I\right)/P\left(O_2^{II}\right)\right]\right) \qquad (5)$$

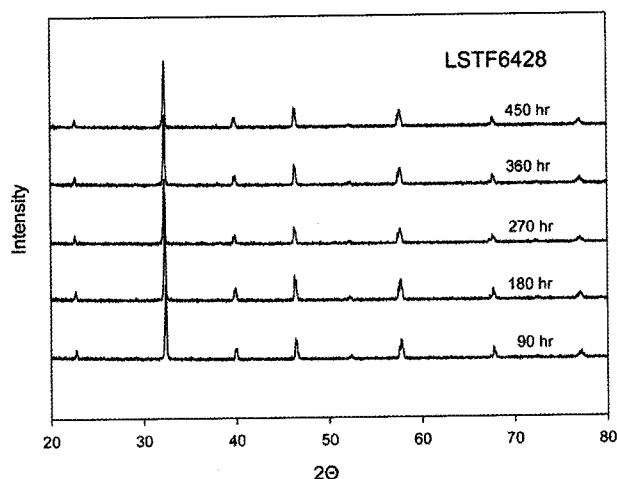**Fig. 10.** XRD analysis of $La_{0.6}Sr_{0.4}Ti_{0.2}Fe_{0.8}O_{3-\delta}$ powder sintered 1,573 K after long-term phase stability test in He atmosphere at 1,173 K.

Where F is Faraday's constant, J is oxygen flux (in A/cm^2), t is membrane thickness, R is gas constant, T is absolute temperature, and $P\left(O_2^I\right)$ and $P\left(O_2^{II}\right)$ are the oxygen partial pressures on the feed and sweep side of the surface of the membranes, respectively.

Ionic conductivity of the $La_{0.6}Sr_{0.4}Ti_{0.2}Fe_{0.8}O_{3-\delta}$ membrane was calculated from the measured oxygen permeation flux using equation (5). Fig. 8 showed the Arrhenius plots calculated from the ionic conductivity as function of temperature.

The apparent activation energy was calculated from the Arrhenius plot of ionic conductivity as function of reciprocal temperature (1/T (K)). The apparent activation energy was 80.5 kJ/mol between 1,073 and 1,223 K temperature range. The activation energies for ionic conduction are similar in magnitude to that of LSCF membranes, Taraoka *et al.* reported from 64 to 86 kJ/mol [24].

3.4. Chemical Stability

Fig. 9. shows the X-ray diffraction pattern of $La_{0.6}Sr_{0.4}Ti_{0.2}Fe_{0.8}O_{3-\delta}$ membrane before and after oxygen permeation test for 40 h. There were no observation of peaks of second phase on both feed side and permeate side.

Fig. 10. shows the X-ray diffraction pattern of

La$_{0.6}$Sr$_{0.4}$Ti$_{0.2}$Fe$_{0.8}$O$_{3-\delta}$ powder after long-term stability test with various time durations in He atmosphere at 1,173 K.

There was no observation of second peaks even after 450 h. This shows La$_{0.6}$Sr$_{0.4}$Ti$_{0.2}$Fe$_{0.8}$O$_{3-\delta}$ membrane has excellent phase stability at high temperature and low oxygen partial pressure.

4. Conclusions

La$_{0.6}$Sr$_{0.4}$Ti$_{0.2}$Fe$_{0.8}$O$_{3-\delta}$ ceramic powders have successfully synthesized via polymerized complex method using citric acid as the chelating agent. The single perovskite oxide was obtained even at calcinations temperature 1,073 K. The discontinuity in the dilatometric curve was observed at 1,003 K. The thermal expansion coefficients of La$_{0.6}$Sr$_{0.4}$Ti$_{0.2}$Fe$_{0.8}$O$_{3-\delta}$ were 21.19 × 10^{-6}/ K from 473 to 1,273 K, which is lower thermal expansion coefficient comparing LSCF series. The total conductivity and electric conductivity depending on oxygen partial pressure studied in the oxygen partial pressure range, 2.1 × 10^{-3}~0.21 atm. The electrical conductivities of the La$_{0.6}$Sr$_{0.4}$Ti$_{0.2}$Fe$_{0.8}$O$_{3-\delta}$ increased to a maximum at 823 K, kept plateau until 923 K, and then started to decrease from 1,003 K. The total conductivity showed predominantly p-type electronic in the oxygen partial pressure range. The oxygen flux of La$_{0.6}$Sr$_{0.4}$Ti$_{0.2}$Fe$_{0.8}$O$_{3-\delta}$ membrane increased with increasing temperature, and the oxygen permeation flux through 1.6 mm membrane exposed to flowing air (P$_h$ = 0.21 atm) and helium (P$_l$ = 0.037 atm) was 0.17 mL/cm^2 · min at 1,223 K. The activation energy of ionic conductivity calculated from oxygen permeation flux of La$_{0.6}$Sr$_{0.4}$Ti$_{0.2}$Fe$_{0.8}$O$_{3-\delta}$ membrane was calculated to be 80.5 kJ/mol. The long-term stability test with various time durations in He atmosphere at 1,173 K confirmed no phase change even after 450 h, displaying excellent phase stability of La$_{0.6}$Sr$_{0.4}$Ti$_{0.2}$Fe$_{0.8}$O$_{3-\delta}$ membrane.

References

1. J. E. ten Elshof, H. J. M. Bouwmeester, and H. Verweij, "Oxidative coupling of methane in a mixed-conducting perovskite membrane reactor", *Appl. Catal. A.*, **130**, 195 (1995).

2. Y. Zeng, Y. S. Lin, and S. L. Swartz, "Perovskite-type ceramic membrane: synthesis, oxygen permeation and membrane reactor performance for oxidative coupling of methane", *J. Membr. Sci.*, **150**, 87 (1998).

3. C. H. Chen, H. Bouwmeester, R. H. E. V. Doors, H. Kruidhof, and A. J. Burggraaf, "Oxygen permeation of La$_{0.3}$Sr$_{0.7}$CoO$_{3-\delta}$", *Solid State Ionics*, **98**, 7 (1997).

4. T. M. Gur, A. Belzner, and R. A. Huggins, "A new class of oxygen selective chemically driven nonporous ceramic membranes. Part I. A-site doped perovskites", *J. Membr. Sci.*, **75**, 151 (1992).

5. V. V. Kharton, E. N. Naumovich, and A. V. Nikolaev, "Materials of high-temperature electrochemical oxygen membranes", *J. Membr. Sci.*, **111**, 149 (1996).

6. L. Qiu, T. H. Lee, L. M. Liu, Y. L. Yang, and A. J. Jacobson, "Oxygen permeation studies of SrCo$_{0.8}$Fe$_{0.2}$O$_{3-\delta}$", *Solid State Ionics*, **76**, 321 (1995).

7. L. W. Tai, M. M. Nasrallah, H. U. Anderson, D. M. Sparlin, and S. R. Sehlin, "Structure and electrical properties of La$_{1-x}$Sr$_x$Co$_{1-y}$Fe$_y$O$_3$. Part 1. The system La$_{0.8}$Sr$_{0.2}$Co$_{1-y}$Fe$_y$O$_3$", *Solid State Ionics*, **76**, 259 (1995).

8. J. H. Park and J. P. Kim, "Properties according to Sr substitution into La$_{1-x}$Sr$_x$Co$_{0.2}$Fe$_{0.8}$O$_{3-\delta}$", Proc.

1st Symp. of the membrane society of Korean, Eds. N. W. Kim and J. H. Kim, pp. 180, Yong-In, Korea.

9. Y. Teraoka, H. M. Zhang, S. Furukawa, and N. Yamazoe, "Oxygen permeation through perovskite-type oxides", *Chem. Lett.*, **1743** (1985).

10. R. Bredesen and J. Sogge, In *A technical and economic assessment of membrane reactors for hydrogen and syngas production*, In seminar on the Ecological Applications of Innovative Membrane technology in the chemical Industry, Cerato, Calabria, Italy, 1996.

11. J. E. ten Elshof, H. J. M. Bouwmeester, and H. Verweij, "Oxygen transport through $La_{1-x}Sr_xFeO_{3-\delta}$ membranes. I. Permeation in air/He gradients", *Solid State Ionics*, **81**, 97 (1995).

12. J. W. Stevenson, T. R. Armstrong, R. D. Carmeim, L. R. Pederson, and L. R. Weber, "Electrochemical Properties of Mixed conducting perovskite $La_{1-x}M_xCo_{1-y}Fe_yO_{3-\delta}$ (M = Sr, Ba, Ca)", *J. Electrochem. Soc.*, **143**, 2722 (1996).

13. C. Y. Tsai, A. G. Dixon, Y. H. Ma, W. R. Moser, and M. R. Pascucci, "Dense perovskite $La_{1-x}A_xFe_{1-y}Co_yO_{3-\delta}$ (A = Ba, Sr, Ca), Membrane synthesis, Application and characterization", *J. Am. Ceram. Soc.*, **81**, 1437 (1998).

14. T. J. Mazanec, T. L. Cable, J. G. Frye, and W. R. Kliewer, US patent, 5,591,315 (1997).

15. M. Schwartz, J. H. White, and A. F. Sammells, US patent, 6,214,757 (2001).

16. V. V. Kharton, A. P. Viskup, E. N. Naumovich, and N. M. Lapchuk, "Mixed electronic and ionic conductivity of LaCo(M)O₃ (M = Ga, Cr, Fe or Ni): I. Oxygen transport in perovskites LaCoO₃-LaGaO₃", *Solid State Ionics*, **104**, 67 (1997).

17. V. V. Kharton, A. P. Viskup, D. M. Bochkov, E. N. Naumovich, and O. P. Reut, "Mixed electronic and ionic conductivity of LaCo(M)O₃ (M = Ga, Cr, Fe or Ni): III. Diffusion of oxygen through $LaCo_{1-x-y}Fe_xNi_yO_{3+/-\delta}$ ceramics", *Solid State Ionics*, **110**, 61 (1998).

18. S. J. Benson, D. Waller, and J. A. Kilner, "Degradation of $La_{0.6}Sr_{0.4}Fe_{0.8}Co_{0.2}O_{3-\delta}$ in Carbon Dioxide and water Atmospheres", *J. Electochem. Soc.*, **146**, 1305 (1999).

19. J. H. Park and S. D. Park, "Oxygen Permeability and Structural Stability of $La_{0.6}Sr_{0.4}Co_{0.2}Fe_{0.8}O_{3-\delta}$ Oxygen Membrane", *Korean J. Chem. Eng.*, **24**(5) (2007).

20. A. Yaremchenko, V. V. Kharton, A. L. Shaula, M. V. Patrakeev, and F. M. B. Marques, "Transport properties and thermal expansion of perovskite-like $La_{0.3}Sr_{0.7}Fe(Al,Cr)O_{3-\delta}$ ceramics", *J. Eur. Ceram. Soc.*, **25**, 2603 (2005).

21. E. V. Tsipis, M. V. Patrakeevb, V. V. Kharton, A. A. Yaremchenko, G. C. Mather, A. L. Shaula, I. A. Leonidov, V. L. Kozhevnikov, and J. R. Fradea, "Transport properties and thermal expansion of Ti-substituted $La_{1-x}Sr_xFeO_{3-\delta}$ (x = 0.5 ~0.7)", *Solid State Sciences*, **7**, 355 (2005).

22. R. D. Shannon, "Revised effective ionic radii and systematic studies of interatomic distances in halides and chalcogenides", *Acta Crystallogr.*, **A32**, 751 (1976).

23. S. Kim, Y. L. Yang, R. Christoffersen, and A. J. Jacobson, "Oxygen permeation, electrical conductivity and stability of the perovskite oxide $La_{0.2}Sr_{0.8}Cu_{0.4}Co_{0.6}O_3-O_{3-\delta}$", *Solid State Ionics*, **104**, 57 (1997).

24. Y. Teraoka, H. Zhang, K. Okamoto, and N. Yamazoe, "Mixed Ionic-electronic conductivity of $La_{1-x}Sr_xCo_{1-y}Fe_yO_{3-\delta}$ perovskite-type oxides", *Mat. Res. Bull.*, **23**, 51 (1988).